Energy Reports 4 (2018) 507–519

Contents lists available at ScienceDirect

Energy Reports

journal homepage: www.elsevier.com/locate/egyr

Research paper

Design of a MW-scale thermo-chemical energy storage reactor

Michael Angerer [a,*], Moritz Becker [a], Stefan Härzschel [a], Konstantin Kröper [a], Stephan Gleis [a], Annelies Vandersickel [a], Hartmut Spliethoff [a,b]

[a] Technical University of Munich, Department of Mechanical Engineering, Institute for Energy Systems, 85748 Garching, Germany
[b] ZAE Bayern, 85748 Garching, Germany

HIGHLIGHTS

- A novel design for a MW-scale fluidized bed thermochemical storage is developed.
- Proof of concept is achieved by experimental pretests.
- A model of the reactor design is build using clustered CSTRs.
- A power output of 15 MW can be expected from 100 m^3 bed volume.
- The reactor performance is limited by heat transfer.

ARTICLE INFO

Article history:
Received 28 May 2018
Accepted 20 July 2018
Available online 22 August 2018

Keywords:
Thermal energy storage
$CaO/Ca(OH)_2$
Fluidized bed
Large scale

ABSTRACT

The reversible exothermic reaction of CaO with water is considered one of the most promising reactions for high temperature thermal energy storage. In this paper, a novel technical design of a MW-scale thermochemical energy storage reactor for this reaction is presented. The aim is to provide an easy, modular and scalable reactor, suitable for industrial scale application. The reactor concept features a bubbling fluidized bed with a continuous, guided solid flow and immersed heat exchanger tubes. To investigate the reactor design, a model is build using clustered CSTRs. The technical feasibility of the concept is proven in experimental tests, which are also used to identify key parameters of the model. Fluidization of the fine $CaO/Ca(OH)_2$ powder was found to be challenging, but problems were overcome using mild calcination conditions and a special gas distributor plate. Using the model, it is found, that a thermal power of 15 MW can be expected from a reactor volume of 100 m^3. To study influences of different parameters on the reactor model performance, a sensitivity analysis is carried out and heat transfer between the reactor and the immersed heat exchangers is found to have by far the largest influence and the reaction system performance. Future research should therefore focus more on heat transfer.

1. Introduction

In recent years, the mitigation of climate change and thus the de-carbonization of energy supply systems has become a major goal worldwide (United Nations, 2015). Yet, most sources of renewable energy are fluctuating, resulting in an increasing need for energy storage systems. Alongside electricity storage, heat storage is going to play an important role in the transformation of today's energy system as it is in many cases more efficient and cheaper than electricity storage (Mathiesen et al., 2015; Connolly et al., 2014; Lund et al., 2016).

Thermal energy storage can be subdivided into sensible, latent and chemical storage (Dinçer and Rosen, 2011). The former is in commercial operation in various applications (e.g. Dinter and Gonzalez, 2014; Tian and Zhao, 2013), while the latter two are currently mainly subject of research (Zalba et al., 2003; Pardo et al., 2014b; Prieto et al., 2016; Cot-Gores et al., 2012). This paper presents a storage system using the reversible chemical reaction of calcium oxide with steam:

$$CaO\,(s) + H_2O(g) \leftrightarrow Ca(OH)_2(s)\ \Delta H_R = -104\ \text{kJ/mol} \quad (1)$$

The predominant advantages of this system are the extremely low storage material costs (~ 0.15 €/kWh) (Angerer et al., 2018) combined with the ability to store heat without losses over long periods. This makes the system suitable for large scale and long-term energy storage. A reactor should hence be designed to make use of these advantages. Therefore, the goal of the present work is to design a reactor system for the gas–solid reaction (1) that:

* Corresponding author.
E-mail address: michael.angerer@tum.de (M. Angerer).

https://doi.org/10.1016/j.egyr.2018.07.005

Nomenclature

Abbreviations

CSTR	Continuous stirred tank reactor
DSC	Differential scanning calorimetry
FBR	Fluidized bed reactor
FM	Fluidization medium
g	gaseous
WF	Working fluid (Heat transfer fluid, in this case: water)
TGA	Thermogravimetric analysis

Chemical Formulas

CaO	Calcium oxide
$Ca(OH)_2$	Calcium hydroxide
H_2O	Water

Latin Symbols

A	Surface area (m^2)
d	Characteristic particle diameter (μm)
g	Gravitational acceleration (m/s^2)
h	Enthalpy (kJ/kg)
H	Height (m)
ΔH_r	Reaction enthalpy (kJ/kmol)
k	Heat transfer coefficient (kW/m^2 K)
l	Length (m)
m	Mass (kg)
$\dot{m}$	Mass flow rate (kg/s)
M	Molar mass (kg/kmol)
n	Mole (kmol)
p	Pressure (bar)
$\dot{Q}$	Heat flow (kW)
r	Reaction rate (kmol/s)
t	Time (s)
T	Temperature (in °C if not specified otherwise) (°C)
v	Superficial gas velocity (on empty vessel basis) (m/s)
X	Mole content of $Ca(OH)_2$ (mol/mol)

Subscripts

B	Bed
Bu	Bulk
$dehy$	Dehydration
eq	Equilibrium
F	Filter
FM	Fluidization medium
GDP	Gas distributor plate
H	Heater
hy	Hydration
in	Inlet
out	outlet
R	Reactor
S	Solids
w	Weight
WF	Working fluid

- is scalable into multi-MW-scale and
- enables a separation of storage power and capacity.

There are many possible applications for efficient and cheap high temperature energy storage with different requirements and specifications. The most prominent case is probably solar thermal power generation (Tian and Zhao, 2013; Schmidt and Linder, 2017). Flexibilization of conventional power plants (Angerer et al., 2018) and power-to-heat are two additional ones. Even domestic applications were proposed (Schmidt and Linder, 2016). In the author's opinion, power-to-heat may be the most promising application; therefore, charging using electrical heating of the system is also discussed in this paper.

Reaction (1) was first proposed for energy storage purposes in the 1970s (Wentworth and Chen, 1976; Ervin, 1977). Yet up to now no commercial systems are available and the technology is still in a development stage (Pardo et al., 2014b; Cot-Gores et al., 2012). During the last years, research has been intensified and various lab scale reactors and corresponding models were developed. An overview thereof is presented in Table 1. A review on the topic was recently published by Pan and Zhao (Pan and Zhao, 2017).

In general there are four types of reactors available for gas–solid reactions:

- Fixed bed reactors
- Moving bed reactors
- Fluidized bed reactors (FBR)
- Entrained flow reactors

Fixed bed reactors are the most common setup in lab scale test rigs (e.g. Schaube et al., 2013a; Yan and Zhao, 2016; Schmidt et al., 2017; Linder et al., 2014; Schmidt et al., 2014; Fujii et al., 1985, compare Table 1), how ether, they come with the disadvantage of discontinuous operation while the other concepts allow for continuous operation. Entrained flow reactors are unfeasible, as they require rather large amounts of carrier gas and a larger reactor volume compared to the other types. A moving bed reactor was proposed by Schmidt et al. (2015). This concept has some advantages, e.g. no carrier gas is necessary, but the operation is difficult as the unmodified fine powders have a very low flowability. Up to now, successful operation of a moving bed reactor over a multitude of cycles has not been reported.

FBRs have the advantage of better heat and mass transfer compared to moving bed reactors and require significantly lower gas velocities compared to entrained flow reactors, therefore they have been widely proposed for thermochemical energy storage (e.g. Criado et al., 2017; Flegkas et al., 2018; Rougé S et al., 2017; Criado et al., 2014a). It is reported, that the fluidization of the fine $CaO/Ca(OH)_2$ powder is difficult, yet successful fluidization of $CaO/Ca(OH)_2$ using additives or modified particles has been reported (Criado et al., 2017; Rougé S et al., 2017; Pardo et al., 2014a).

As mentioned, up to now only lab scale reactors with outputs <10 kW_{ch} have been set up and to the best of our knowledge, no detailed concepts for large-scale reactors have been proposed.

On the modeling side, detailed models of fixed bed reactors have been developed (Ströhle et al., 2014; Nagel et al., 2014). For FBRs, Ostermeier et al. developed a model for the gas distributor plate used in the system presented here with detailed hydrodynamics but without heat transfer and chemical reaction and validated it against cold model experiments (Ostermeier et al., 2017). Meanwhile Criado set up simple models to recalculate experiments in two kW-scale test rigs at CEA (Criado et al., 2017; Rougé S et al., 2017; Pardo et al., 2014a). These models feature a K–L-approach for bubbling fluidized beds according to Kunii and Levenspiel (1991), but do not solve a heat balance. Instead, temperature is given as an input from the measurements (Criado et al., 2017, 2014a). A very sophisticated model for a FBR with the thermochemical reaction system $MgO/Mg(OH)_2$ was recently published by Flegkas et al. (2018). This model features bundled tube heat exchangers in combination with a K–L modeling approach.

Alongside the development of reactors, the reaction kinetics (Criado et al., 2014b; Schaube et al., 2012) and cycling stability (Nagel et al., 2014; Schaube et al., 2012; Lin et al., 2009) have

Table 1
Lab-scale reactors and models of $CaO/Ca(OH)_2$ storage systems.

Type of reactor	Heat transfer	Experimental	Models
Fixed bed	Direct heat transfer	Schaube et al. (2013a) and Yan and Zhao (2016)	Schaube et al. (2013b) and Ströhle et al. (2014)
	Indirect heat transfer	Schmidt et al. (2017), Linder et al. (2014), Schmidt et al. (2014) and Fujii et al. (1985)	Nagel et al. (2014)
Moving bed	Indirect heat transfer	Schmidt et al. (2015)	–
Fluidized bed	Indirect heat transfer	Criado et al. (2017), Rougé S et al. (2017) and Pardo et al. (2014a)	Criado et al. (2017), Flegkas et al. (2018), Criado et al. (2014a) and Ostermeier et al. (2017)

been investigated. The chemical reaction for both hydration and dehydration is rather fast and the material shows complete conversion over a multitude of cycles. However, it is reported, that with cycling, the compressive strength of the particles decreased (Lin et al., 2009) and refinement of the particle size occurred (Schaube et al., 2012).

FBR designs with a strong focus on heat transfer between the bed and heat exchangers have previously been developed for other applications. Closest related to the design presented here are applications for indirect thermal storage using sand (Steiner et al., 2016; Schwaiger et al., 2014; Haider et al., 2012) and drying of moist lignite (Hoehne et al., 2009; Schreiber et al., 2011). For both applications, large scale fluidized beds with bundled tube heat exchangers are used. The fluidized bed lignite dryer at the Niederaußem power plant reaches a heat transfer of 75 MW (Hoehne et al., 2009) while the sandTES pilot facility reaches a power in- or output of 280 kW (Steiner et al., 2016).

Related to these concepts, this article presents a FBR design for large-scale thermochemical energy storage alongside a simple modeling approach to identify key influence parameters on the reactor performance. The model is taking into account chemical kinetics as well as heat transfer and different flow schemes within the reactor design and is backed by experimental investigations to identify model parameters.

Section 2 details the proposed reactor design of an industrial scale thermochemical energy storage FBR. In Section 3, the modeling of the reactor is explained. As fluidization of pure, unmodified industrial grade CaO, as used in the reactor concept proposed in this paper, has not yet been reported in literature, Section 4 briefly summarizes some experimental pretests to demonstrate the technical feasibility of the concept and identify key parameters of the model. The model is the used in Section 5 to investigate geometry and flow setup of the reactor as well as to identify crucial parameters and bottlenecks of the system.

2. Conceptual design of a MW-scale reactor

The main task of the reactor concept is to bring the solid $CaO/Ca(OH)_2$ particles in contact with the gaseous reaction partner. The second task is to efficiently supply or remove heat at an appropriate temperature level for the chemical reaction from the bed and transfer it to a heat transfer medium that is not in direct contact with the bed.

2.1. Reactor type

Looking at the overall investment costs of the storage system, it is clear, that the storage material which is available on industrial scale at ∼0.15 €/kWh (Angerer et al., 2018) plays a minor role. The majority of the costs is due to the reactor and heat transfer system. To keep costs for applications with high storage capacity low, it is mandatory to separate the expensive heat exchangers from the cheap storage capacity. This can be accomplished by continuously passing the storage material through a reactor as shown in Fig. 1. This is not possible in fixed bed reactors, leaving moving- and fluidized-bed reactors as well as entrained flow reactors as possible concepts. Due to the advantages in heat and mass transfer and the superior material handling characteristics, a fluidized bed is chosen in this work as the most promising reactor concept for large scale applications.

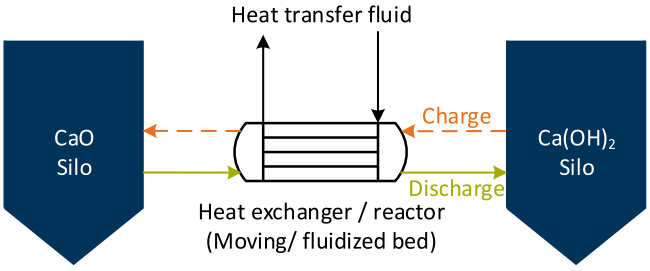

Fig. 1. Scheme of a thermochemical storage system with separation of power (heat exchanger/reactor) and capacity (silos).

2.2. Reactor and heat exchanger design

The conceptual design of the reactor is shown in Fig. 2. The fluidized bed is operated as a dense bubbling bed. A special gas distributor plate with a high number of nozzles is used to distribute the fluidization gas uniformly over the reactor cross section. The nozzles are inducing the gas with high velocity and turbulence in horizontal direction, reducing channeling and agglomeration. A more detailed description of the gas distributor plate can be found in Ostermeier et al. (2017). The overall fluidization velocity is moderate and should be reduced as far as possible to minimize the parasitic influence of pressure losses.

To keep the fine storage material within the reactor and have a rather clean fluidization gas at the exit, a high temperature filter system is used. Temperatures in the reactor are estimated in a range between 400 and 700 °C. Therefore a sintered metal filter system is suitable. These filters can be cleaned periodically by reverse flow pressure impulses, keeping even the fine fraction of the storage material within the hot reactor volume.

To improve the residence time distribution, baffles are integrated in the bed leading to a guided flow of solids from inlet to outlet. As proposed by Steiner et al. (2016), additional "gas cushions" can be used to assist the directed solid flow through the reactor. The material input can be done by screw feeders (as demonstrated in Schmidt et al., 2015), the outlet by overflow. The reactor is separated from the storage silo by gas-locks.

Up to now, fluidization in lab scale setups was achieved in a mixture of steam and air/nitrogen (Criado et al., 2017, 2014a). During charging operation, steam is released due to reaction (1). This steam contains roughly 40% of the energy required for charging, mostly in the form of condensation heat of this steam. It is thus clear, that this energy needs to be utilized to set up an efficient system integration (as shown e.g. in Angerer et al., 2018; Schmidt and Linder, 2016). If this steam is found in a mixture with air/nitrogen, condensation is not possible at constant temperatures and, depending on steam content and overall pressure, is shifted towards low temperatures. To make efficient use of the condensation energy, it is therefore mandatory to operate the fluidized

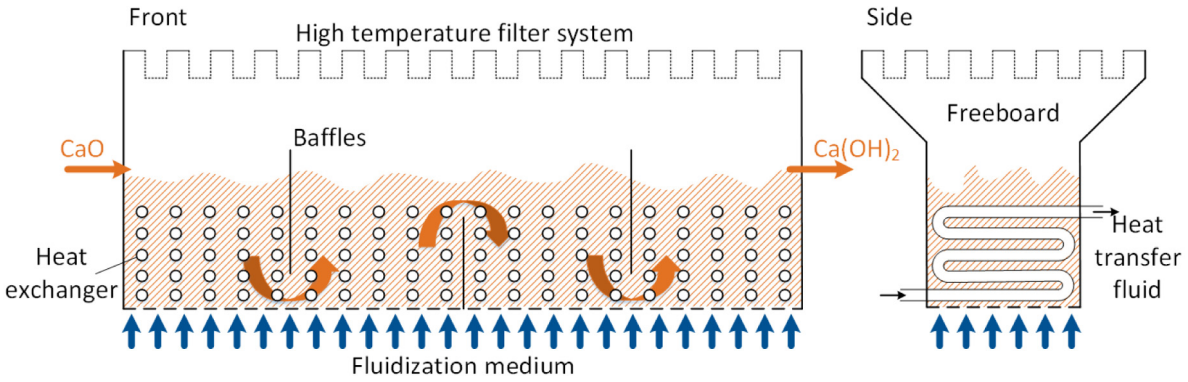

Fig. 2. Reactor design of a continuous MW-scale FBR for thermochemical energy storage.

bed (including filters and gas-locks) in pure steam atmosphere as explained in Angerer et al. (2018). The bed can even be operated at elevated pressures to increase the condensation temperature level, if this is useful for the system integration.

The most efficient way to transfer heat from (discharging) or into (charging) the bed is by bundled tube heat exchangers. The heat transfer coefficient for surfaces inside the bed is approximately four times as high as for surfaces in the freeboard above the bed (Kunii and Levenspiel, 1991). In fluidized bed combustion, this is often not possible due to abrasive ash components. As no abrasion is expected with the fine CaO/$Ca(OH)_2$ particles, heat exchangers in the form of bundled tubes are placed directly inside the bed. The heat exchanger tubes are packed into the bed as dense as possible, as long as fluidization is not negatively affected. Fig. 2 shows an in-line configuration of the heat exchanger tubes with multiple passes and in- and outlets through the reactor sides. It is possible that other configurations like staggered arrangement or u-elbows with in- and outlet from the reactor top are more advantageous, but these questions are beyond the scope of this work.

The most prominent application for the discharging operation is live steam generation. Therefore, in discharging mode, the heat exchanger is used as a steam generator. This steam generator is operated as a once-through boiler. This sets higher requirements to feed water quality, but ensures a much more advantageous part load behavior. With a circulation boiler, part load could only be achieved by reducing bed height, while in a once-through boiler it can be controlled by the feed water mass flow rate.

As it can be seen from Fig. 2, the system is easily scalable. Length, width and number of baffles can be adapted to find a suitable storage design. The reactor can also be used in a modular setup. Reactors can be clustered in parallel or even serial setup, using the same fluidization medium (FM) in multiple reactor stages.

3. Modeling

To investigate the reactor design, a model is developed. The aim of the model is not to investigate characteristics of the fluidized bed in detail, but to provide a simple and transparent approach to:

- Identify bottlenecks and crucial parameters of the system design and thus guide further research
- Provide a reactor model for the investigation of the integration into larger energy systems

For bubbling fluidized beds, so called K–L-models are popular (Criado et al., 2017; Flegkas et al., 2018; Kunii and Levenspiel, 1991). These models split the reactor into two homogeneous phases: a lean phase (bubbles) and a dense phase (emulsion). The dense and the lean phase exchange heat and mass with each other.

As the K–L-model is a mass transfer model, it is particularly necessary, if the composition of the gas phase can be different in bubbles and emulsion (e.g. if due to reaction (1) water vapor is removed inside the emulsion leaving only inert carrier gas behind, reducing the water partial pressure and thus the reaction rate). Recent system integration studies have shown that it is highly recommended to use pure steam as fluidization medium to reach higher system efficiencies (Angerer et al., 2018; Schmidt and Linder, 2017). Therefore, the reactor concept presented here is operated with a homogeneous steam atmosphere and no difference in water partial pressure is expected within the reactor. Thus, the only impact of a K–L-model would be the possibility of different temperatures in bubbles and emulsion. In well fluidized beds, it is often assumed, that gas and particle temperature are homogeneous. Applying this assumption, the K–L-model can be reduced to a continuously stirred tank (CSTR) model without any disadvantages in model quality. In conclusion, the main assumptions of the model are:

- The solid holdup in the reactor is homogeneous (no local discretization, perfect mixing)
- Gas and solids in the reactor have the same temperature (no temperature distribution)
- The model is stationary (no startup or shutdown procedures, no time discretization)

3.1. CSTR single reactor model

A scheme of the reactor model is shown in Fig. 3. Two different cases are distinguished; case A) with heat exchangers in the bed and a working fluid (WF, indexed with W) flowing through these heat exchangers and case B) with electrical heaters with a fixed surface temperature T_H inside the bed.

The overall mass conservation of the reactor can be written as:

$$\dot{m}_{S,in} + \dot{m}_{FM,in} = \dot{m}_{S,out} + \dot{m}_{FM,out} \tag{2}$$

With $\dot{m}_{FM}$ being the mass flow rate of the FM and $\dot{m}_S$ the mass flow rate of the solids consisting of CaO and $Ca(OH)_2$:

$$\dot{m}_S = \dot{m}_{CaO} + \dot{m}_{Ca(OH)_2} \tag{3}$$

The conversion X is defined as the molar share of $Ca(OH)_2$ in the reactor:

$$X = n_{Ca(OH)_2}/n_{S,R} \tag{4}$$

Consequently the mass fraction of $Ca(OH)_2$ in the reactor is defined as:

$$X_w = m_{Ca(OH)_2}/m_{S,R} \tag{5}$$

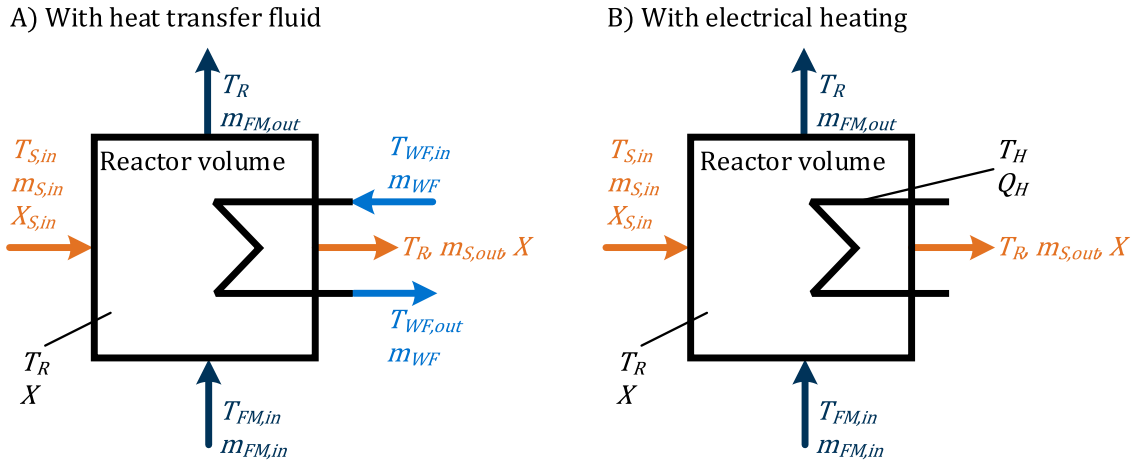

Fig. 3. Fig. 3: Schema mapping of the reactor system.

The reaction rate can be calculated from the kinetic rate equation dX/dt as:

$$r = \frac{dX}{dt} \cdot n_{S,R} \tag{6}$$

With $n_{S,R}$ being the molar holdup of solids in the reactor volume and dX/dt being the experimentally determined kinetic rate equation. The molar holdup is calculated from the bed volume using the bed density in fluidized state ρ_R. It is assumed, that the reactor has a square cross section with the length l_R.

$$n_{S,R} = V_B \cdot \frac{\rho_R}{M_{S,R}} = H_B \cdot l_R^2 \cdot \frac{\rho_R}{M_{S,R}} \tag{7}$$

H_B is the bed height in fluidized state and $M_{S,R}$ the average molar mass of the solids in the reactor. The bed density ρ_R is calculated from the bulk densities $\rho_{Bu,i}$ of CaO and $Ca(OH)_2$ and the measured bed expansion H_B/H_{Bu}, which was found to be similar for pure CaO and $Ca(OH)_2$ fluidized beds.

$$\rho_R = \frac{\left(\rho_{Bu,Ca(OH)2} \cdot X_w + \rho_{Bu,CaO} \cdot (1 - X_w)\right)}{H_B/H_{Bu}} \tag{8}$$

The kinetic rate equation dX/dt depends on several parameters:

$$\frac{dX}{dt} = f(T_R, p_{H2O}, X) \tag{9}$$

As the reactor is operated in pure steam, the steam partial pressure is the same as the reactor pressure. It is assumed, that the pressure losses in the reactor are mainly due to the gas distributor plate, which is situated at the inlet of control volume covered by the model. Thus the steam partial pressure in the reactor is:

$$p_{H2O} = p_R = p_{FM,in} - \Delta p_{GDP} - \rho_R \cdot g \cdot H_B \tag{10}$$

Due to the filters downstream the reactor an additional pressure loss is induced resulting in a lower pressure at the reactor exit:

$$p_{FM,out} = p_R - \Delta p_F \tag{11}$$

The mass balance for e.g. CaO can be written as:

$$\dot{m}_{S,in} \cdot \frac{X_{S,in}}{M_{S,in}} + r = \dot{m}_{S,out} \cdot \frac{X}{M_{S,R}} \tag{12}$$

The energy balance of the reactor can be written as:

$$\begin{aligned} &\dot{m}_{S,in} \cdot h_{S,in} + \dot{m}_{FM,in} \cdot h_{FM,in} + k \cdot A \cdot \Delta T_{log} \\ &\quad = \dot{m}_{S,out} \cdot h_{S,out} + \dot{m}_{FM,out} \cdot h_{FM,out} + r \cdot \Delta H_r \end{aligned} \tag{13}$$

The enthalpies at the inlet depend on the temperatures of the inlet mass flows:

$$h_{S,in} = f\left(T_{S,in}\right) \text{ and } h_{FM,in} = f\left(T_{FM,in}\right) \tag{14}$$

While the enthalpies at the outlet depend on the homogeneous reactor temperature:

$$h_{S,out} = f\left(T_R\right) \text{ and } h_{FM,out} = f\left(T_R\right) \tag{15}$$

All enthalpies and heat capacities are calculated using data from the NIST chemistry webbook (NIST, 0000). The heat of reaction ΔH_r is calculated according to Kirchhoff's law, using the same dataset. The mass flow of the FM at the inlet is calculated from the superficial gas velocity:

$$\dot{m}_{FM,in} = v_{FM,in} \cdot \rho_{FM,in} \text{ with } \rho_{FM,in} = f(p_R, T_{FM,in}) \tag{16}$$

The temperature difference between the reactor and the heat exchanger surface is calculated as:

$$\Delta T_{log} = \frac{T_{WF,in} - T_{WF,out}}{\log\left(\frac{T_R - T_{WF,in}}{T_R - T_{WF,out}}\right)} \tag{17}$$

If the reactor is heated by an electric heater with constant temperature T_H, the temperature difference can be simplified:

$$\Delta T_{log} = T_H - T_R \tag{18}$$

Finally, the energy balance for the WF inside the heat exchanger can be written as:

$$\dot{m}_{WF} \cdot h_{w,in} = \dot{m}_{WF} \cdot h_{w,out} + k \cdot A \cdot \Delta T_{log} \tag{19}$$

In case of electrical heating, this can again be simplified to:

$$\dot{Q}_H = k \cdot A \cdot \Delta T_{log} \tag{20}$$

Overall, in case of heat transfer from a WF, the independent Eq. (12), (13) and (19) are found to describe the three independent variables X, T_R and $T_{WF,out}$. In case of electrical heating, there are only two independent Eqs. (12) and (13) describing X and T_R. However, the result is a nonlinear system of equations that is solved using MATLAB's (Mathworks Inc, 0000) lsqnonlin-solver.

3.2. Clustering of CSTRs and model of the complete reactor design

In Fig. 2, several baffles are shown to create a distinct flow of the solids through the FBR. To account for this in the reactor model, each reactor section between two baffles is represented by one CSTR model. Fig. 4 shows a setup of two reactors with three baffles (as shown in Fig. 2) in a countercurrent setup of solids and WF modeled using 8 CSTRs. The FM of the first reactor (first row of CSTR) is collected and used again in the second reactor stage. In this

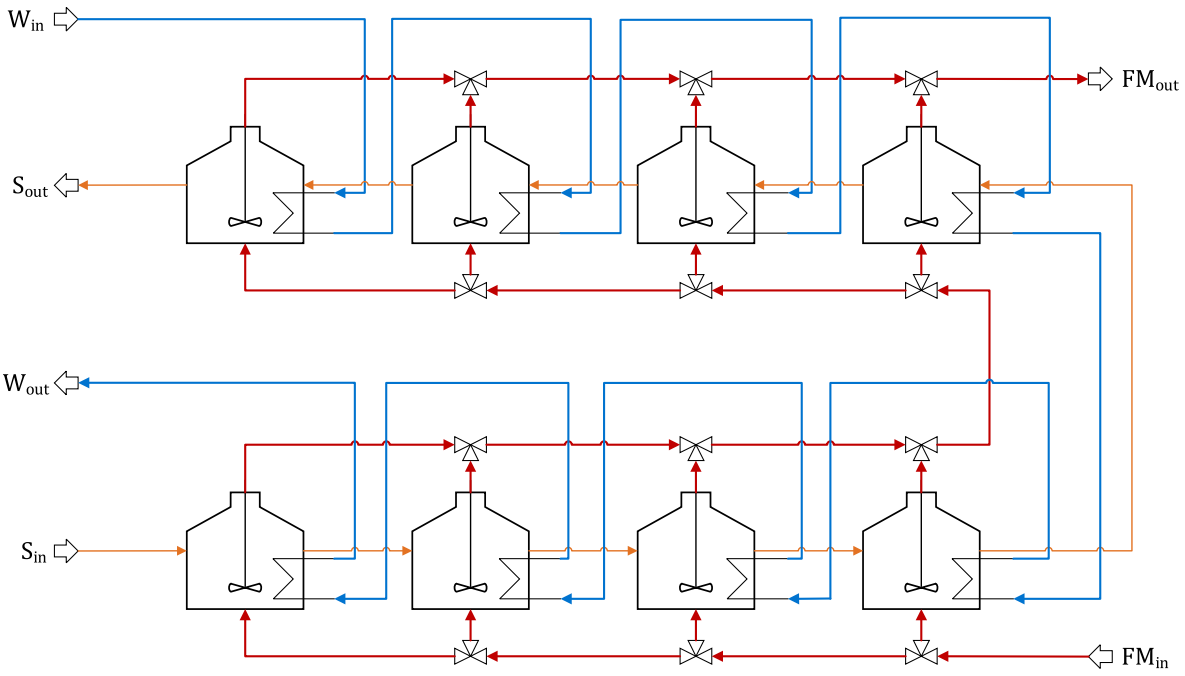

Fig. 4. Modeling scheme of two reactors (with three baffles each) in a countercurrent setup resulting in a 2x4 matrix of reactors.

case, the flow scheme between solids and FM is cross-cocurrent. Of course, a cross-countercurrent setup is also possible.

In addition to fluidization, a notable amount of steam is needed to clean the filters at the top of the reactor via reversed flow pressure impulses. In case of the dehydration this sums up to 50 % of the inlet mass flow for fluidization. In case of hydration 25% are needed, as the inlet velocity for hydration is double the velocity for dehydration to compensate for the gas consumption of the chemical reaction. In the model, this is accounted for by adding the FM for the filter cleaning after the reactor. The filter cleaning in downstream reactor stages is also conducted with FM at global inlet conditions (FM_{in}) not with FM at reactor inlet conditions.

In case of a (cross-) cocurrent setup, the calculation can be performed straightforward using the result of one reactor as input of the next reactor. When (cross-)countercurrent flow is applied, an iterative scheme has to be applied. The calculation is done in direction of the solid flow and the results of the previous calculation are used as inputs for the WF and/or FM side. The iterative procedure is repeated until convergence is reached and the sum of the absolute enthalpy differences between the current and the last iteration is below 0.5 kJ/kg (corresponds to approx. 0.02% of the total value).

4. Experimental pretests and identification of key model parameters

As mentioned before, fluidization has already been successfully demonstrated using a large share of easy-to-fluidize particles (Pardo et al., 2014a) or particles calcined with high temperatures resulting in reduced reactivity (Criado et al., 2017). The aim of the concept presented here is to use pure commercial CaO calcined under moderate conditions, thus providing higher reactivity. To identify key parameters for the simulations described in chapter 3, a number of pretests are conducted.

4.1. Characterization of the storage material

Throughout this study, as storage material, commercial $Ca(OH)_2$ (Weißfeinkalkhydrat CL-90 S according to DIN EN 459-1) and industrial grade $CaCO_3$ provided by Märker Kalk GmbH from a mine in Harburg, Germany is used. The $Ca(OH)_2$ is used for the investigation of the reaction kinetics. The $CaCO_3$ is calcined under moderate conditions in a lab furnace without purge gas at 800 °C for 48 h, reaching full technical conversion to CaO. The material is cycled in a fixed bed reactor to investigate the mechanical stability (Becker et al., 2018). Cycling is done close to equilibrium conditions in pure steam atmosphere at 1.5 bar absolute pressure by alternating the steam feed temperature between 400 °C (hydration) and 600 °C (dehydration). Table 2 shows characteristic values of the particle size distribution. The moderate reaction conditions can also be expected in fluidized bed systems and lead to a high mechanical cycling stability of the particles. The decreasing value of d_{10} indicates that fines are formed during cycling, jet this seems to happen to a much lower extent compared to harsh reaction conditions further from equilibrium as reported in literature (Criado et al., 2014b; Schaube et al., 2012; Lin et al., 2009). On the other hand, the increasing value of d_{90} proves that agglomeration takes place as well under the mentioned reaction conditions. Further investigation of the matter is necessary especially concerning attrition during fluidized bed cycling, but the particles show a substantially higher mechanical cycling stability than reported in Criado et al. (2014b), Schaube et al. (2012) and Lin et al. (2009). Pardo (2013) investigated reaction cycles in a fluidized bed reactor in a mixture of nitrogen and steam using a similar material. He found that during 15 cycles slight agglomeration took place and the amount of fines was reduced.

Table 2
Characteristic particle diameters (on particle volume base) of the industrial grade $CaCO_3$ and CaO gained from that material (Becker et al., 2018).

	d_{10} in µm	d_{50} in µm	d_{90} in µm
$CaCO_3$	212.2	350.7	495.3
CaO after calcination	174.6	345.5	496.6
CaO after 4 cycles	165.9	385.5	563.8

4.2. Chemical equilibrium and reaction kinetics

Several authors have investigated equilibrium and kinetics of reaction (1) (Criado et al., 2014b; Schaube et al., 2012; Matsuda et

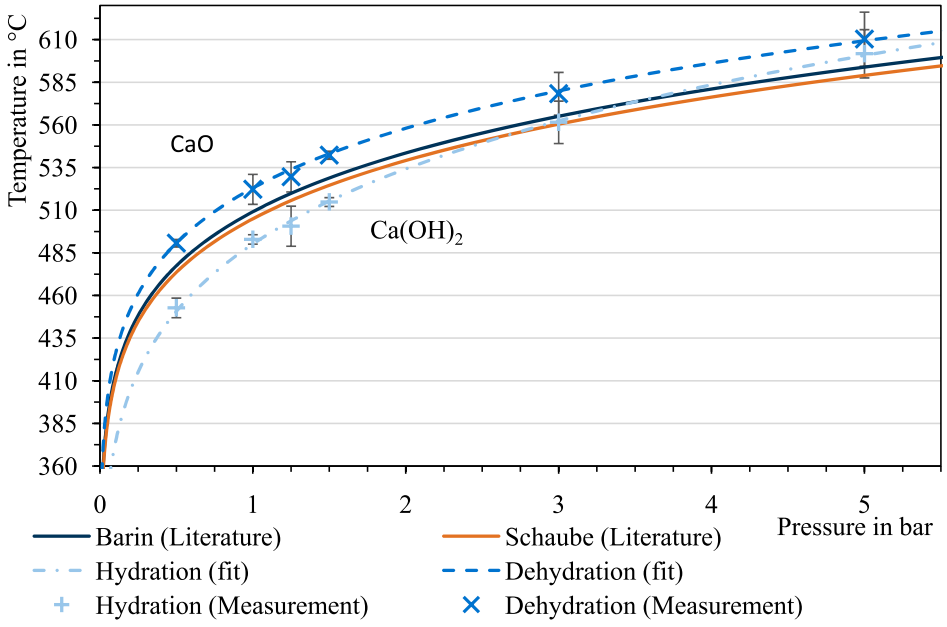

Fig. 5. Measured onset temperatures (with 95% confidence range) for the hydration and dehydration and resulting Eqs. (21) and (22) in comparison with literature equilibrium curves from Barin (2008) and Schaube et al., (2012).

al., 1985). However, most of the measurements used in these publications were conducted in mixed steam/nitrogen atmosphere, resulting in absolute steam pressures below 1 bar. As the operation of the reactor presented in this work is expected at steam pressures $\geq$1 bar, it is necessary to provide suitable kinetic data for this range. Therefore, own measurements in a TGA/DSC with 5 mg material in pure steam atmosphere between 0.5 and 5 bar were conducted.

A theoretical equilibrium curve can be calculated from thermochemical data from Barin (2008). Literature is not conclusive about whether a hysteresis can be expected for reaction (1). Samms and Evans (1968) as well as Halstead and Moore (1957) proposed no hysteresis, looking at their measurement data, a slight hysteresis especially for low steam pressures might be visible. Matsuda et al. (1985) found a strong hysteresis in their measurements (Matsuda et al., 1985). In the data of Schaube et al. (2012), a hysteresis is visible, jet it is neglected in the discussion and an inaccuracy of the measurement is assumed. The results of this work concerning the chemical equilibrium are shown in Fig. 5. It is not the aim of this paper to discuss the question of a hysteresis of reaction (1). The measurement data indicate, that at least the apparent onset points of the reaction show a certain hysteresis, especially for lower steam pressures. Therefore it was decided, to express the onset of reaction by two separate equations:

$$p_{onset,dehy} = \exp\left(-\frac{13090}{T\,[K]} + 16.443\right) \tag{21}$$

for the dehydration and

$$p_{onset,hy} = \exp\left(-\frac{9713.3}{T\,[K]} + 12.725\right) \tag{22}$$

for the hydration. These curves are not to be understood as a chemical equilibrium with a hysteresis but more like reaction onset points used to describe the apparent reaction kinetics.

The determined rate equations correspond to the second cycle of standard two-cycle measurements, which were conducted for three heating rates (1, 4 and 8 K/min) and at six different vapor pressures (0.5, 1.0, 1.25, 1.5, 3.0 and 5.0 bar). The equations were derived from the measurement data using a genetic algorithm. The equations represent the measurement data with an R_2-value of 95.6% for the Hydration and 98.5% for the dehydration.

The equation gained for the dehydration is:

$$\frac{dX}{dt} = -449974 \cdot \exp\left(-\frac{91282}{8.3145 \cdot T\,[K]}\right) \cdot \left(1 - \min\left\{\frac{1}{\frac{p_{H2O}}{p_{onset,dehy}}}\right\}\right)^{3.47} \cdot X \tag{23}$$

And for the hydration:

$$\frac{dX}{dt} = 390827 \cdot \exp\left(-\frac{87460}{8.3145 \cdot T\,[K]}\right) \cdot \left(\max\left\{\frac{1}{\frac{p_{H2O}}{p_{onset,hy}}}\right\} - 1\right)^{3.43} \cdot (1 - X) \tag{24}$$

4.3. Fluidization and heat transfer

Fluidization of the commercial $Ca(OH)_2$ and $Ca(OH)_2$ produced from industrial grade $CaCO_3$ is tested in a cold model, thoroughly described in Ostermeier et al. (2018). Fig. 6 shows the setup used. It consists of a simple glass cylinder with an inner diameter of 140 mm and an interchangeable gas distributor plate. The heat transfer probe, thoroughly described in Ostermeier et al. (2018), can be removed for pure fluidization tests. Experiments are conducted at atmospheric conditions; the FM is nitrogen at ambient temperature. The key findings of the experiments are:

- Fluidization is possible to some extent even for fine powders using a proprietary gas distributor plate design supplied by SCHWING Technologies GmbH (more difficult with usual perforated plates or steel composite cloth)
- Fluidization works very well with the in-house calcined material described in Table 2 and a bubbling fluidized bed is formed (as can be seen from a video in the supplementary material of the article)

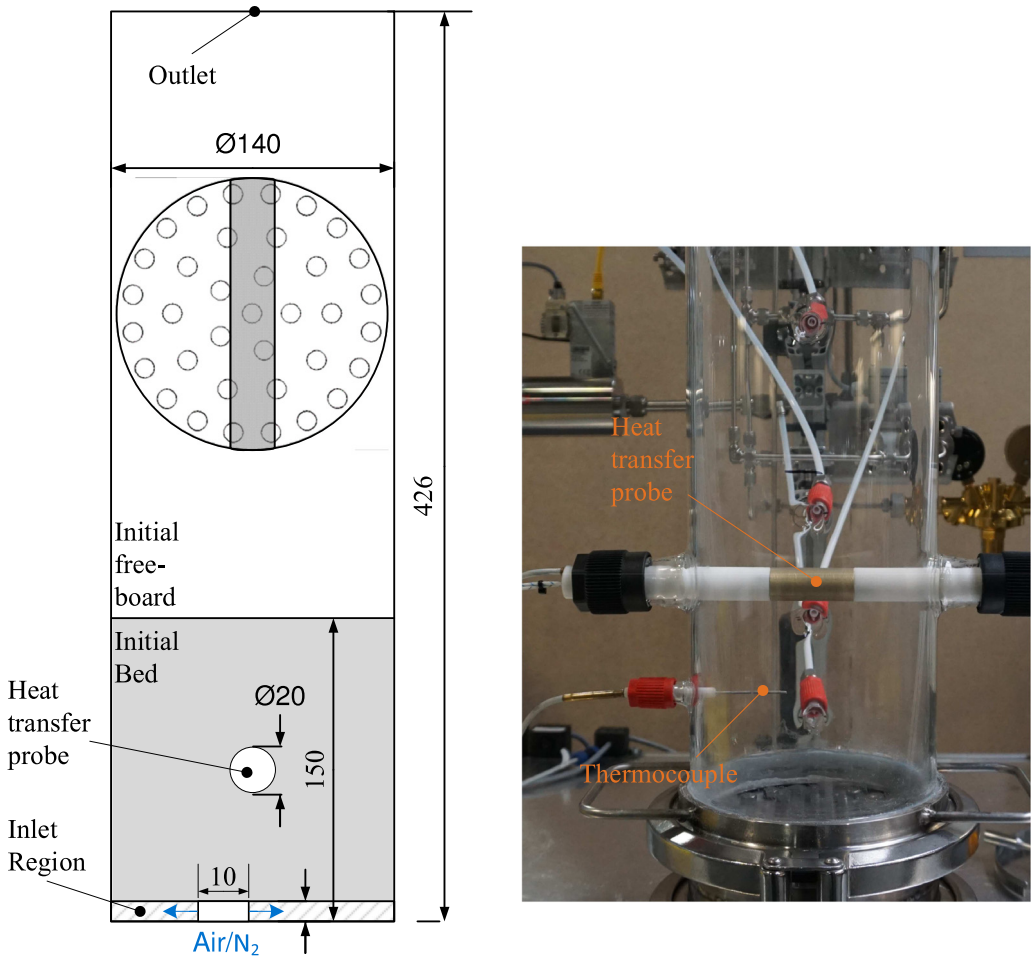

Fig. 6. Setup for experimental fluidization investigation. Air-blown cold fluidization test rig at TUM for fluidization and heat transfer tests, further details in Becker et al. (2018) and Ostermeier et al. (2018).

- Superficial fluidization velocity should range between 0.1 and 0.6 m/s (on empty vessel basis)
- The bed expansion of the bubbling bed at 0.2 m/s is roughly 125%

Footage of the fluidization tests presented at Becker et al. (2018) can be found in the supplementary material of the article.

As the viscosity of hot gases exceeds the viscosity of cold gases, fluidization can be expected to be even better under reactive conditions (Yang, 2003). Hot fluidization under reactive conditions was successfully tested at the facilities of Schwing Technologies GmbH and a 10 kW pilot scale reactor is currently under commissioning at TUM.

The measured heat transfer coefficients for the $Ca(OH)_2$ powders range from 50 to 350 W/m^2 K (Becker et al., 2018), depending on the particle size distribution and thus fluidization quality. For the in-house calcined $CaCO_3$, values of $\sim$ 300 W/m^2 K were measured for fluidization velocities between 0.2 and 0.3 m/s (Becker et al., 2018), thus this value is used in the simulations presented here.

5. Results and discussion

The modeling results shown here account for a fluidized bed volume of 40 m^3. As the freeboard above the bed requires approximately the same volume, the total reactor volume is roughly 100 m^3. Of course, the reactor design and thus the thermal output can easily be scaled by changing the length or width of the reactor or by applying a modular reactor setup. The discharging (hydration) case is discussed with heat exchanger and a WF, while the charging (dehydration) is discussed with electrical heating. Of course, charging with thermal energy transferred from a WF is possible as well, but is not be discussed here for reasons of simplicity.

First the model is used to assess the general reactor performance, then degrees of freedom of the reactor design, like flow setup and number of baffles are investigated. Finally the influence of key parameters on the reactor model performance is investigated using a sensitivity analysis

5.1. Base case and input parameters

The most relevant input parameters are shown in Table 3. They were partly identified in the experiments, described in the previous chapter. For the dehydration a smaller FM inlet velocity is used as additional steam is produced by the reaction and the outlet velocity is higher than the inlet velocity. This results in a lower pressure loss over the gas distributor and a higher relative share of FM necessary for filter cleaning. The electrical heater temperature was chosen at 650 °C so that a specific load of the electrical heaters of 2 W/cm^2 is not exceeded. A bed height of 1.5 m is chosen based on experience of SCHWING Technologies GmbH. The heat transfer surface area results from packing heat exchangers tubes with an outer diameter of 50 mm as close as possible into the bed while leaving 60% of the horizontal and vertical cross section clear for the fluidization. The 40 m^3 of bed volume include both, the volume of the heat exchanger and the bed volume. As a base case, a reactor

Table 3
Input parameters for the reference case simulation.

Parameters identified by experiments		Hydration	Dehydration
Fluidization velocity at inlet $v_{FM,in}$	m/s	0.4	0.15
Pressure loss of gas distributor plate Δp_{GDP}	bar	0.2	0.075
Pressure loss of filter system Δp_F	bar	0.1	0.1
Heat transfer coefficient k	W/m^2 K	300	300
Bulk density of product $\rho_{Bu,i}$	kg/m^3	0.72	0.82
Bed expansion H_B/H_{Bu}	–	1.25	1.25
Other input parameters			
Total bed volume (all reactors)	m^3	40	40
Height of the reactor bed H_B	m	1.5	1.5
Heat transfer surface area (all reactors)	m^2	514.6	514.6
Conversion X at the inlet	–	0.1	0.9
Mass flow of solids $\dot{m}_{S,in}$ at the inlet	kg/s	7	7
Mass flow of WF $\dot{m}_W$	kg/s	6	–
T_S at the inlet	°C	600	350
T_{FM} at the inlet	°C	350	350
P_{FM} at the inlet	bar	1.4	1.4
Inlet temperature of the WF $T_{W,in}$	°C	150	–
Inlet pressure of the WF $p_{W,in}$	bar	100	–
Surface temperature of the electric heaters T_H	°C	–	650
Share of the FM for filter cleaning on each stage	–	0.25	0.5

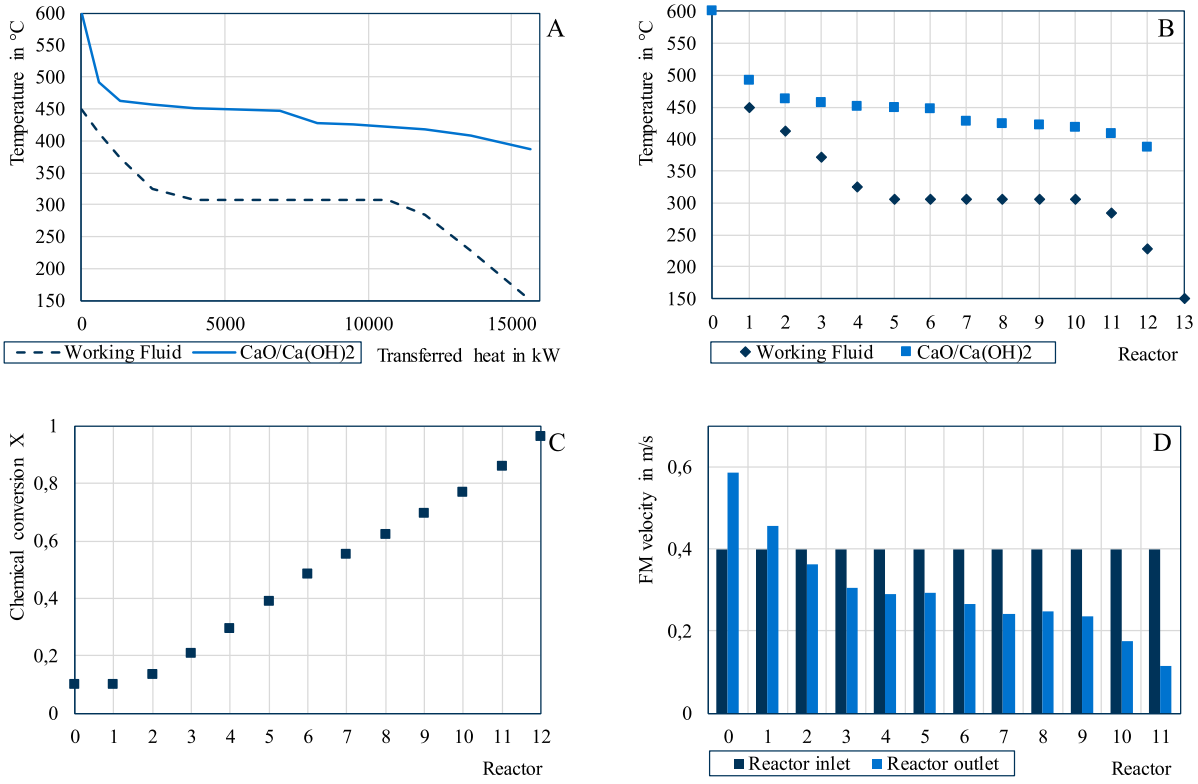

Fig. 7. Results of the reference case simulation of the discharging (hydration, countercurrent flow setup): (A) Q–T-Diagram of the reactor. (B) Temperatures of WF and solid particles at the exit of each of the 12 (6 × 2) reactors. Reactor 0 corresponds to the temperature of the solid inlet (before reactor 1), while reactor 13 corresponds to the inlet temperature of the WF. (C) Conversion at the exit of each reactor. (D) Superficial velocity of the FM at reactor inlet and outlet.

with 5 baffles (6 reactor compartments) and two reactor stages, further denoted as 2 × 6-configuration, is used.

Fig. 7 shows the results of the reference case simulation of the discharging/hydration. The flow setup is countercurrent for the solids and the WF and cross-cocurrent for the solids and the FM, just as shown in Fig. 4. Fig. 7(A) shows the heat–temperature-diagram for the reactor. It can be seen that approximately 15 MW of heat are transferred in the reference case and the WF reaches an outlet temperature of 450 °C. (B) shows the same temperatures, this time over the 12 reactors in the solid flow direction. The solid feed has a temperature of 600 °C and is rapidly cooled to the reaction temperature of <500 °C, which is slightly decreasing over reactors 2–12. A step in the temperature can be seen between reactors 6 and 7, marking the beginning of the second reactor stage with lower pressure (due to pressure losses in the filters of stage one and the GDP of stage two).

At the exit of the reactor, conversion is almost complete (as can be seen in (C)) and thus the solids are slightly cooled down in reactor 12 reaching a solid outlet temperature of 390 °C. By operating the CaO storage at elevated temperatures (in this case 600 °C) and the $Ca(OH)_2$ storage at lower temperatures (in this case 350 °C), the temperature gap is used as a sensitive energy storage and increases the energy density in the material by 20%. Of course, this can only be applied for limited cycle durations (<1

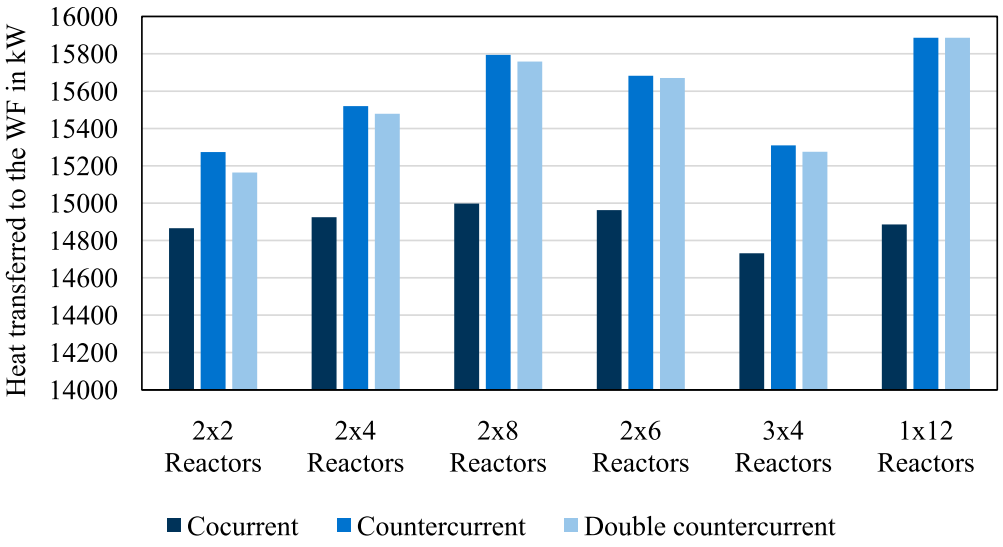

Fig. 8. Heat transferred to the WF (as a measure of the reactor performance) for different reactor setups.

week). For long-term storage, both silos should be operated at ambient temperature and the remaining heat in the product at the reactor exit should be transferred to the feed by additional heat exchangers.

Fig. 7(D) shows the superficial velocities of the FM at the reactor in- and outlet. In the experimental pretests it was found, that fluidization is possible between 0.1 and 0.6 m/s. As steam is consumed by the reaction in case of the hydration, it can be seen that the velocity at the inlet has to be above 0.2 m/s, as the outlet velocity is lower than the inlet velocity. In the first three reactors, this is not the case due the rather low reaction rate and the higher temperatures in these reactors (compare Fig. 7(C) and (B)). Towards the end of the reactor, when temperatures of the solid and thus the fluidization gas drop while the reaction rate is still high, the superficial velocity at the outlet gets critically low. As the flow direction of the solids is from reactor 1 to 12, this can be expected to have a positive effect on the material transport through the baffles as a slight pressure gradient can be expected to be induced by this behavior.

5.2. Influence of the reactor design

For discharging operation, the influence of the reactor design on the heat transferred to the WF is shown in Fig. 8. Three conclusions can be drawn from that figure:

- The cocurrent setup for the solids and the WF has clear disadvantages compared to countercurrent setups. However, the cross-countercurrent setup with regard to the solids and the FM (indicated as 'Double countercurrent') is not advantageous to the cross-cocurrent setup. Furthermore, the cross-cocurrent setup in this case is simpler to implement technically, as the solids do not have to be transported against pressure gradients. Thus, the optimal reactor setup is countercurrent for WF and solids and cross-cocurrent for FM and solids.
- The number of baffles (and thus the number of reactors in a row in the model) has a positive influence on the reactor efficiency. On the other hand, an increasing number of baffles may result in solid transport problems as reported by Steiner et al. (2016). To keep the reactor simple and yet efficient, a number of 3–5 baffles per reactor stage is recommended.
- Finally, the influence of the number of stages is investigated using three different setups of 12 reactors. From Fig. 8, it can be seen that increasing the number of stages causes disadvantages in transferred heat. This can be attributed to the decreasing operation pressure over the reactor stages, resulting in lower reaction temperatures in higher reactor stages and thus lower temperature difference between reactor and WF. How ether, this is only one measure for the reactor performance. Inducing more reactor stages significantly reduces the amount of FM needed, as the FM from lower stages is "reused" in upper stages. In the two stage setup, only 66% and in the three stage setup only 55% of the FM compared to the one stage setup is needed. Depending on the system integration, this may result in a significant reduction of parasitic losses from the compression of the FM. Thus, a setup with two stages is considered a good compromise.

Similar conclusions were found for other cases investigated (electrical and thermal charging), hence the recommendations concerning the reactor design are applicable for these as well. Figures for the electrical dehydration can be found in the supplementary material of the article.

5.3. Sensitivity analysis

To investigate the influence of various model and design parameters on the reactor performance, a sensitivity analysis is carried out. To this end, the parameters are varied with ±25% in steps of 5%, the effect on reactor performance is analyzed and related design trade-offs are discussed. The results for the discharging (Hydration) are shown in Fig. 9. Several conclusions can be drawn:

- The predominant influence is the heat transfer represented by the kA-value. To maximize the performance, the reactor should thus be designed and operated to reach maximum heat transfer. This implies a maximum dense packing of the heat exchanger pipes and optimized fluidization for high heat transfer coefficients. Optimizing design and parameters concerning heat transfer should be a key target of future research.
- In the same context, changes in the pressures of the FM and the WF can be seen. An increase in FM pressure shifts the chemical equilibrium towards higher temperatures and

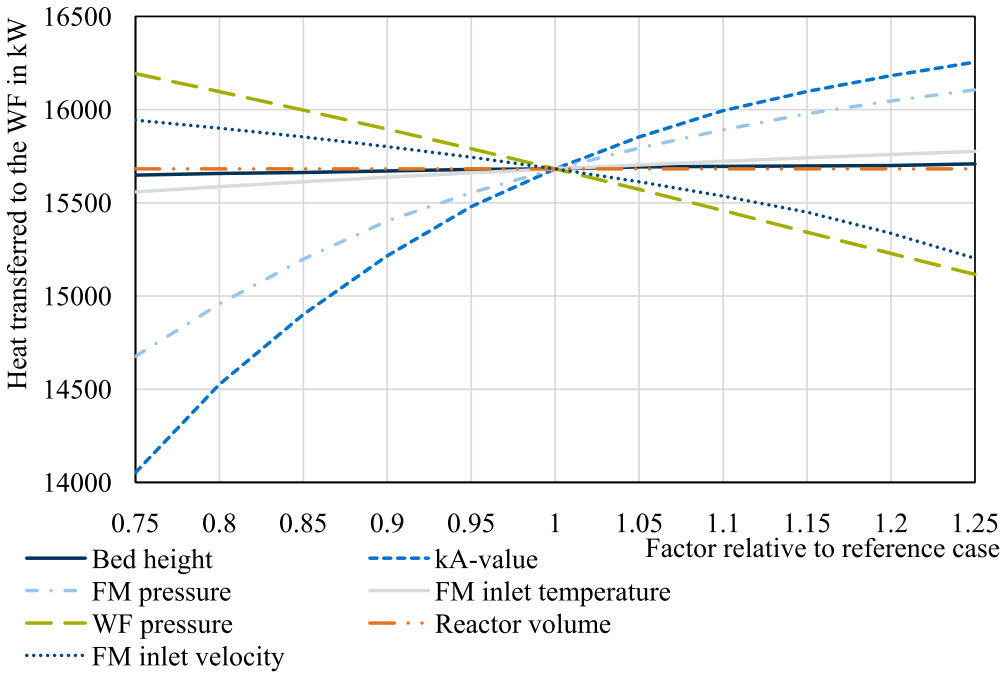

Fig. 9. Sensitivity analysis of the reactor model in discharging mode. All values are modified by ±25% in 5% steps relative to the reference case given in Table 3.

thus increases the reactor temperature and the heat transferred to the WF. The same effect can be observed by decreasing the pressure of the WF. This results in decreasing evaporation temperatures thus increasing the logarithmic temperature difference and the heat transfer.

- Fig. 9, the inlet velocity of the FM should be chosen as low as possible. Anyway, the model does not cover side effects of the FM velocity on the heat transfer. The heat transfer reaches a maximum between 0.2 and 0.3 m/s (Becker et al., 2018). Thus the fluidization velocity should be tuned to reach optimized heat transfer coefficients.
- The reactor volume (and thus the residence time) has a very limited effect on the reactor performance (under the assumption of a constant heat transfer surface area). This leads to the conclusion, that the chemical reaction is sufficiently fast and kinetics have a very limited influence on the reactor performance.
- The FM inlet temperature as well as the bed height have a limited influence on the overall reactor performance.

Fig. 10 shows the sensitivity analysis for the electrically heated charging process. Again, the reaction is comparably fast, so there is almost no influence from the reactor volume. The same accounts for the fluidization medium velocity and temperature and the bed height. Again, side effects of this quantities on the heat transfer coefficient that might occur in reality are not covered by the model. The pressure at which the reaction takes place (FM pressure) has a certain influence as it shifts the temperature of the reaction and thus the driving temperature difference according to Eq. (18). As for the hydration, the heat transfer coefficient has a large influence on the system performance, indication that the system is controlled by heat transfer.

The predominant effect is caused by the heater temperature. This is due to its effect on the temperature difference in Eqs. (13) and (18). As the temperature of the reactor stays rather constant, the heater temperature directly affects the temperature difference. E.g. an increase of 5% in the heater temperature (from 650 to 682.5 °C) increases the temperature difference by 32.5 °C which is approximately 25% of its value. Thus the heater temperature is very important. Technically up to 850 °C are possible using immersion heaters. The heater temperature, that can actually be reached, depends on the fluidization quality. If the fluidization is inhomogeneous, heaters are likely to overheat and fail in zones of low heat transfer. To improve fluidization quality and homogeneity is thus one way to ensure efficient electrical heating. Another way is to have a detailed control system for the heater surface temperatures to adaptively decrease heating power and prevent destruction of the heaters in zones of low heat transfer. Both topics should be in the focus of future research.

6. Conclusion and outlook

In this work, a novel concept for a MW-scale fluidized bed thermochemical energy storage reactor using the reaction of CaO with steam is presented. During preliminary experimental tests, the fluidization of pure commercial $CaO/Ca(OH)_2$ powder proved to be challenging, however this was overcome by using a special, proprietary gas distributor plate and in house calcined CaO. Further pretests, including TGA/DSC measurements to identify reaction kinetics, heat transfer measurements, hot and cold fluidization tests, were carried out to identify key parameters of the system. Based on these findings, a reactor concept for a large-scale storage reactor is derived and a clustered-CSTR model of this reactor design is implemented in MATLAB.

Using this model, parameter- and sensitivity studies are performed and recommendations and trade-offs to be considered during reactor design are elaborated. It is found that with the given assumptions, a 40 m^3 bed (corresponding to approx. 100 m^3 of total reactor volume) can deliver a power output of approximately 15 MW, generating steam at 100 bar/450 °C in discharging. The heat transfer between the fluidized bed and the WF is found to have by far the largest influence on the reactor performance, indicating that heat transfer controls the reaction in an industrial scale reactor, not chemical kinetics, or mass transfer as suggested in literature (e.g. Criado et al., 2017) for lab scale setups. For electrical charging, a 40 m^3 bed can be used as well to reach approximately the same flow of $CaO/Ca(OH)_2$. In this case, heat transfer and the heater temperature are the main influence parameters.

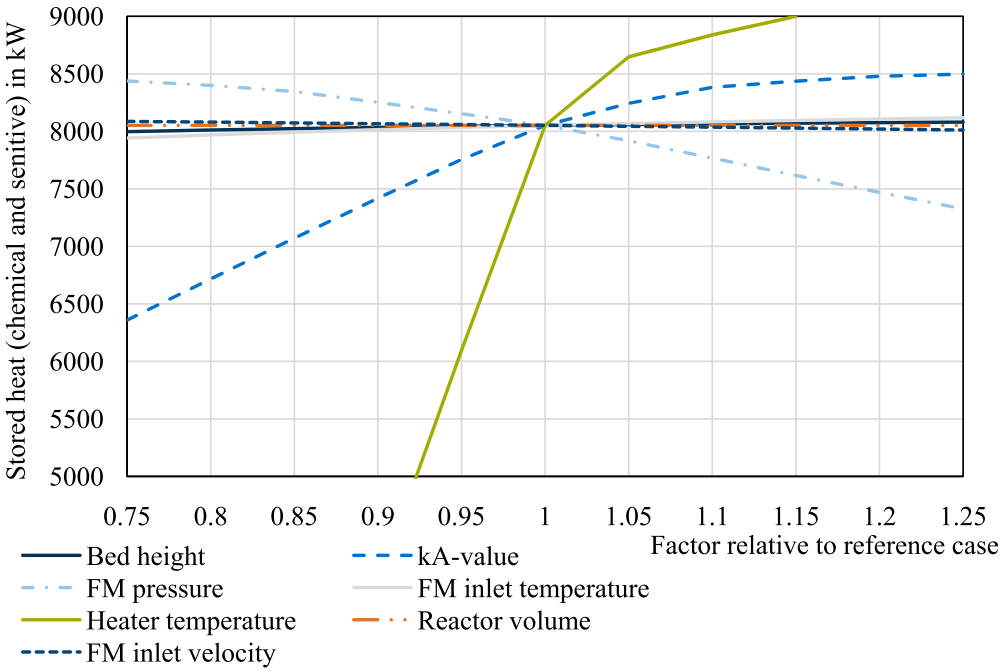

Fig. 10. Sensitivity analysis of the reactor model in charging mode. All values are modified by ±25% in 5% steps relative to the reference case given in Table 3.

Results herein indicate that heat transfer is dominating an industrial scale reactor design. It is recommended to focus further research on heat transfer between the fine powder and heat exchangers emerged in the fluidized bed, as this topic is not broadly discussed for the $CaO/Ca(OH)_2$thermochemical storage system in literature (e.g. Criado et al., 2017; Rougé et al., 2017; Pardo et al., 2014a). Alongside the heat transfer, further research is necessary to identify ideal fluidization conditions to maximize heat transfer while minimizing parasitic losses, and improve the storage materials cycling stability and physical properties required for fluidization.

The reactor design and modeling approach presented here is also suitable for other reaction systems like $MgO/Mg(OH)_2$ if these are operated in pure steam atmosphere. The model itself can be used to analyze the integration of the storage into larger energy systems to identify possible applications in industry and power generation.

Acknowledgments

The authors would like to thank Märker Kalk GmbH for providing materials and assistance, and SCHWING Technologies GmbH for providing the gas distributor plate design, a facility for pretests and assistance with the reactor design. This research is part of the project 'Thermochemischer Energiespeicher für thermische Kraftwerke und industrielle Wärme' and is funded by the German Federal Ministry of Economic Affairs and Energy (BMWi) under the funding code 03ET7025 according to a decision of the German Federal Parliament. This work was supported by the German Research Foundation (DFG) and the Technical University of Munich (TUM) in the framework of the Open Access Publishing Program.

Appendix A. Supplementary data

Supplementary material related to this article can be found online at https://doi.org/10.1016/j.egyr.2018.07.005.

References

Angerer, M., Djukow, M., Riedl, K., Gleis, S., Spliethoff, H., 2018. Simulation of cogeneration-combined cycle plant flexibilization by thermochemical energy storage. J. Energy Resour. Technol. 140 (2), 20909.

Barin, I., 2008. Thermochemical data of pure substances. Weinheim u.a.: VCH-Verl.-Ges.

Becker, M., Würth, M., Angerer, M., Härzschel, S., Gleis, S., Vandersickel, A., et al., 2018. Thermochemical Energy Storage with CaO/Ca(OH)2–Development of a Continuous Fluidized Bed Reactor. Düsseldorf.

Connolly, D., Lund, H., Mathiesen, B.V., Werner, S., Möller, B., Persson, U., et al., 2014. Heat roadmap europe: Combining district heating with heat savings to decarbonise the EU energy system. Energy Policy 65, 475–489.

Cot-Gores, J., Castell, A., Cabeza, L.F., 2012. Thermochemical energy storage and conversion: A-state-of-the-art review of the experimental research under practical conditions. Renewable Sustainable Energy Rev. 16 (7), 5207–5224.

Criado, Y.A., Alonso, M., Abanades, J.C., Anxionnaz-Minvielle, Z., 2014. Conceptual process design of a CaO/Ca(OH)2 thermochemical energy storage system using fluidized bed reactors. Appl. Therm. Eng. 73 (1), 1085–1092.

Criado, Y.A., Alonso, M., Abanades, J., Carlos, , 2014. Kinetics of the CaO/Ca(OH)2 hydration/dehydration reaction for thermochemical energy storage applications. Ind. Eng. Chem. Res. 53 (32), 12594–12601.

Criado, Y.A., Huille, A., Rougé, S., Abanades, J.C., 2017. Experimental investigation and model validation of a CaO/Ca(OH)2 fluidized bed reactor for thermochemical energy storage applications. Chem. Eng. J. 313, 1194–1205.

Dinçer, İ., Rosen, M.A., 2011. Thermal Energy Storage: Systems and Applications, second ed. Wiley, Hoboken, N.J.

Dinter, F., Gonzalez, D.M., 2014. Operability, reliability and economic benefits of CSP with thermal energy storage: First year of operation of ANDASOL 3. Energy Procedia 49, 2472–2481.

Ervin, G., 1977. Solar heat storage using chemical reactions. J. Solid State Chem. 22 (1), 51–61.

Flegkas, S., Birkelbach, F., Winter, F., Freiberger, N., Werner, A., 2018. Fluidized bed reactors for solid-gas thermochemical energy storage concepts - Modelling and process limitations. Energy 143, 615–623.

Fujii, I., Tsuchiya, K., Higano, M., Yamada, J., 1985. Studies of an energy storage system by use of the reversible chemical reaction: CaO + H2O ⇌ Ca(OH)2. Sol. Energy 34 (4–5), 367–377.

Haider, M., Schwaiger, K., Holzleithner, F., Eisl, R., 2012. A comparison between passive regenerative and active fluidized bed thermal energy storage systems. J. Phys.: Conf. Ser. 395 (1), 12053.

Halstead, P.E., Moore, A.E., 1957. 769. The thermal dissociation of calcium hydroxide. J. Chem. Soc. 3873.

Hoehne, O., Lechner, S., Schreiber, M., Krautz, H.J., 2009. Drying of lignite in a pressurized steam fluidized bed - theory and experiments. Drying Technol. 28 (1), 5–19.

Kunii, D., Levenspiel, O., 1991. Fluidization Engineering, second ed. Butterworth-Heinemann.
Lin, S., Wang, Y., Suzuki, Y., 2009. High-temperature CaO hydration/Ca(OH)2 decomposition over a multitude of cycles. Energy Fuels 23 (6), 2855–2861.
Linder, M., Roßkopf, C., Schmidt, M., Wörner, A., 2014. Thermochemical energy storage in kW-scale based on CaO/Ca(OH)2. Energy Procedia 49, 888–897.
Lund, H., Østergaard, P.A., Connolly, D., Ridjan, I., Mathiesen, B.V., Hvelplund, F., et al., 2016. Energy storage and smart energy systems. Int. J. Sustainable Energy Plann. Manage. 11, 3–14.
Mathiesen, B.V., Lund, H., Connolly, D., Wenzel, H., Østergaard, P.A., Möller, B., et al., 2015. Smart energy systems for coherent 100% renewable energy and transport solutions. Appl. Energy 145, 139–154.
Mathworks Inc. 0000. MATLAB. [January 05, 2017]; Available from: http://de.mathworks.com/products/matlab/.
Matsuda, H., Ishizu, T., Lee, S.K., Hasatani, M., 1985. Kinetic study of Ca(OH)2/CaO reversible thermochemical reaction for thermal energy storage by means of chemical reaction. Kagaku Kogaku Ronbunshu 11 (5), 542–548.
Nagel, T., Shao, H., Roßkopf, C., Linder, M., Wörner, A., Kolditz, O., 2014. The influence of gas–solid reaction kinetics in models of thermochemical heat storage under monotonic and cyclic loading. Appl. Energy 136, 289–302.
National Institute of Standards andTechnology. 0000. NIST Chemistry WebBook: NIST Standard Reference Database. [January 05, 2017]; Available from: http://webbook.nist.gov/chemistry/.
Ostermeier, P., Vandersickel, A., Becker, M., Gleis, S., Spliethoff, H., 2018. Hydrodynamics and heat transfer around a horizontal tube immersed in a Geldart b bubbling fluidized bed. Int. J. Comput. Methods Exp. Meas. 6 (1), 71–85.
Ostermeier, P., Vandersickel, A., Gleis, S., Spliethoff, H., 2017. Three dimensional multi fluid modeling of Geldart B bubbling fluidized bed with complex inlet geometries. Powder Technol. 312, 89–102.
Pan, Z.H., Zhao, C.Y., 2017. Gas–solid thermochemical heat storage reactors for high-temperature applications. Energy 130, 155–173.
Pardo, P., 2013. Développement d'un procédé de stockage d'énergie thermique haute température par voie thermochimique. Dissertation.
Pardo, P., Anxionnaz-Minvielle, Z., Rougé, S., Cognet, P., Cabassud, M., 2014. Ca(OH)2/CaO reversible reaction in a fluidized bed reactor for thermochemical heat storage. Sol. Energy 107 (0), 605–616.
Pardo, P., Deydier, A., Anxionnaz-Minvielle, Z., Rougé, S., Cabassud, M., Cognet, P., 2014. A review on high temperature thermochemical heat energy storage. Renewable Sustainable Energy Rev. 32 (0), 591–610.
Prieto, C., Cooper, P., Fernández, A.I., Cabeza, L.F., 2016. Review of technology: Thermochemical energy storage for concentrated solar power plants. Renewable Sustainable Energy Rev. 60, 909–929.
Rougé, S.A., Criado, Y., Soriano, O., Abanades, J.C., 2017. Continuous CaO/Ca(OH) 2 fluidized bed reactor for energy storage: First experimental results and reactor model validation. Ind. Eng. Chem. Res. 56 (4), 844–852.
Samms, J.A.C., Evans, B.E., 1968. Thermal dissociation of Ca(OH)2 at elevated pressures. J. Appl. Chem. 18 (1), 5–8.
Schaube, F., Koch, L., Wörner, A., Müller-Steinhagen, H., 2012. A thermodynamic and kinetic study of the de- and rehydration of Ca(OH)2 at high H2O partial pressures for thermo-chemical heat storage. Thermochim. Acta 538, 9–20.
Schaube, F., Kohzer, A., Schütz, J., Wörner, A., Müller-Steinhagen, H., 2013. De- and rehydration of Ca(OH)2 in a reactor with direct heat transfer for thermochemical heat storage. Part A Experimental results. Chem. Eng. Res. Des. 91 (5), 856–864.
Schaube, F., Utz, I., Wörner, A., Müller-Steinhagen, H., 2013. De- and rehydration of Ca(OH)2 in a reactor with direct heat transfer for thermo-chemical heat storage. Part B: Validation of model. Chem. Eng. Res. Des. 91 (5), 865–873.
Schmidt, M., Gollsch, M., Giger, F., Grün, M., Linder, M., 2015. Development of a moving bed pilot plant for thermochemical energy storage with CaO/Ca(OH)2. In: SolarPACES, p. 50041.
Schmidt, M., Gutierrez, A., Linder, M., 2017. Thermochemical energy storage with CaO/Ca(OH)2–Experimental investigation of the thermal capability at low vapor pressures in a lab scale reactor. Appl. Energy 188, 672–681.
Schmidt, M., Linder, M., 2016. Thermochemische energiespeicherung zum saisonalen ausgleich zwischen stromangebot und heizwärmebedarf. Chem. Ing. Tech. 88 (9), 1267.
Schmidt, M., Linder, M., 2017. Power generation based on the Ca(OH) 2 / CaO thermochemical storage system–Experimental investigation of discharge operation modes in lab scale and corresponding conceptual process design. Appl. Energy 203, 594–607.
Schmidt, M., Szczukowski, C., Roßkopf, C., Linder, M., Wörner, A., 2014. Experimental results of a 10-KW high temperature thermochemical storage reactor based on calcium hydroxide. Appl. Therm. Eng. 62 (2), 553–559.
Schreiber, M., Asegehegn, T.W., Krautz, H.J., 2011. Numerical and experimental investigation of bubbling gas - solid fluidized beds with dense immersed tube bundles. Ind. Eng. Chem. Res. 50 (12), 7653–7666.
Schwaiger, K., Haider, M., Hämmerle, M., Wünsch, D., Obermaier, M., Beck, M., et al., 2014. sandTES–an active thermal energy storage system based on the fluidization of powders. Energy Procedia 49, 983–992.
Steiner, P., Schwaiger, K., Walter, H., Haider, M., 2016. Active fluidized bed technology used for thermal energy storage. In: Proceedings of the ASME 10th International Conference on Energy Sustainability - 2016: Presented at ASME 2016 10th International Conference on Energy Sustainability, June 26-30, 2016. The American Society of Mechanical Engineers, Charlotte, North Carolina, USA. New York, N.Y., V001T05A001.
Ströhle, S., Haselbacher, A., Jovanovic, Z.R., Steinfeld, A., 2014. Transient discrete-granule packed-bed reactor model for thermochemical energy storage. Chem. Eng. Sci. 117, 465–478.
Tian, Y., Zhao, C.Y., 2013. A review of solar collectors and thermal energy storage in solar thermal applications. Appl. Energy 104, 538–553.
United Nations. 2015. Paris Agreement. [June 12, 2017]; Available from: http://unfccc.int/files/essential_background/convention/application/pdf/english_paris_agreement.pdf.
Wentworth, W.E., Chen, E., 1976. Simple thermal decomposition reactions for storage of solar thermal energy. Sol. Energy 18 (3), 205–214.
Yan, J., Zhao, C.Y., 2016. Experimental study of CaO/Ca(OH)2 in a fixed-bed reactor for thermochemical heat storage. Appl. Energy 175, 277–284.
Yang, W.-C. (Ed.), 2003. Handbook of Fluidization and Fluid-Particle Systems. Dekker CRC Press, New York NY u.a.
Zalba, B., Marín, J.M., Cabeza, L.F., Mehling, H., 2003. Review on thermal energy storage with phase change Materials, heat transfer analysis and applications. Appl. Therm. Eng. 23 (3), 251–283.